Electronic Supplementary Information

Facile synthesis of novel lithium β-diketonate glyme adducts: the effect of molecular engineering on the thermal properties

Nishant Peddagopu,[a] Patrizia Rossi,[b] Carmela Bonaccorso,[c] Ausrine Bartasyte,[d] Paola Paoli,[b] and Graziella Malandrino, [a,*]

[a.] Dipartimento di Scienze Chimiche, Università di Catania and INSTM UdR Catania, V.le Andrea Doria 6, 95125 Catania, Italy.
[b.] Dipartimento di Ingegneria Industriale, Università di Firenze, Via Santa Marta 3, 50136 Firenze, Italy.
[c.] Dipartimento di Scienze Chimiche, Università di Catania, V.le Andrea Doria 6, 95125 Catania, Italy.
[d.] FEMTO-ST Institute, University of Bourgogne Franche-Comté CNRS UMR 6174, 26 Rue de l'Epitaphe, F-25030 Besançon, France

Table of Contents

Experimental section.

Starting materials: The monohydrate lithium hydroxide [Li(OH)•H_2O, >98%] and 1,1,1,5,5,5-hexafluoro-2,4-pentanedione (H-hfa, >98%), were purchased from Strem Chemicals and used as received. Monoglyme (1,2-Dimethoxyethane, 99.5%), diglyme (bis(2-methoxyethyl)ether, 99.5%), triglyme (2,5,8,11-tetraoxadodecane, >98%), tetraglyme (2,5,8,11,14-pentaoxapentadecane, >99%), dichloromethane (CH_2Cl_2, >99.5%) and n-pentane were purchased from Sigma Aldrich.

Characterization of precursors. Elemental microanalysis was performed using a Carlo Erba 1106 elemental analyser. Fourier Transform Infrared (FT-IR) spectra were recorded using a Jasco FT/IR-430 spectrometer with nujol mulls between NaCl plates. Melting points were taken on very small single crystals using a Kofler hot-stage microscope. Thermogravimetric analyses were made using a Mettler Toledo TGA2 and the STAR^e software. Dynamic thermal analyses were carried out under purified nitrogen flow (50 sccm) at atmospheric pressure with a 5 °C min^{-1} heating rate. Weights of the samples were between 7–10 mg. Differential scanning calorimetry analyses were carried out using a Mettler Toledo Star System DSC 3 under purified nitrogen flow (30 sccm) at atmospheric pressure with a 5 °C/min heating rate. Weights of the samples were between 5-8 mg. NMR experiments were carried out at 27 °C using a 500 MHz spectrometer (^{1}H at 499.88 MHz, ^{13}C NMR at 125.7 MHz) equipped with a pulse field gradient module (Z axis) and a tunable 5mm Varian inverse detection probe (ID-PFG); chemical shifts (δ) are expressed in ppm and are referenced to residual deuterated solvent. NMR data were processed using the MestReC software.

Synthesis of [Li_{12}(hfa)$_{12}$•monoglyme•4H_2O] (1). The Li(OH)•H_2O (0.385 g, 9.18 mmol) 30% excess was first suspended in dichloromethane (40 mL) followed by monoglyme (0.636 g, 7.06 mmol) and finally Hhfa (1.47 g, 7.06 mmol) were added after 10 min and the mixture was refluxed under stirring for 1 h. The excess of LiOH was filtered off. The colorless crystals precipitated after partial evaporation of the solvent. The crystals were collected, washed with pentane, filtered, and dried under vacuum. The reaction yield was 70%. The crude product did not melt up to 220 °C using the Kofler hot-stage microscope (760 Torr). NMR analysis reports: δ_H (500 MHz, CD_3CN, 27 °C) 5.88 (s, 12H, CH_{HFA}) 3.49 (s, 4H, CH_2), 3.32 (s, 6H, OCH_3) ppm; δ_C (125 MHz, CD_3CN, 27 °C) 176.02 (q, CO_{HFA}, ^2J(C,F)=32.4 Hz), 118.08 (q, $CF_{3\ HFA}$, ^1J(C,F)=287.5 Hz), 86.59 (CH_2), 71.38 (CH_2), 57.89 (CH_3) ppm. Elemental analysis for **1** ($Li_{12}C_{64}H_{30}F_{72}O_{30}$): Calc: C, 28.36; H, 1.11. Found: C, 28.21; H, 1.09.

Synthesis of [Li_2(hfa)$_2$•diglyme•H_2O] (2). The Li(OH)·H_2O (0.385 g, 9.18 mmol) 30% excess was first suspended in dichloromethane (40 mL) followed by diglyme (0.473 g, 3.53 mmol) and finally Hhfa (1.47 g, 7.06 mmol) were added after 10 min and the mixture was refluxed under stirring for 1 h. The excess of LiOH was filtered off. The colorless crystals precipitated after partial evaporation of the solvent. The crystals were collected, washed with pentane, filtered, and dried under vacuum.

The reaction yield was 86%. The melting point of the crude product was 80-82°C (760 Torr). NMR analysis reports: δ_H (500 MHz, CD_3CN, 27 °C) 5.88 (s, 2H, CH_{HFA}), 3.61 (m, 4H, CH_2), 3.52 (m, 4H, CH_2), 3.32 (s, 6H, OCH_3) ppm; δ_C (125 MHz, CD_3CN, 27 °C) 176.01 (q, CO_{HFA}, ^2J(C,F)=32.5 Hz), 118.10 (q, $CF_{3\ HFA}$, ^1J(C,F)=287.5 Hz), 86.54 (CH_2), 71.09 (CH_2), 69.53 (CH_2), 57.92 (CH_3) ppm. Elemental analysis for **2** ($Li_2C_{16}H_{18}F_{12}O_8$): Calc: C, 33.13; H, 3.10. Found: C, 33.24; H, 3.14

Synthesis of Li(hfa)•triglyme (3). The Li(OH)•H_2O (0.385 g, 9.18 mmol) 30% excess was first suspended in dichloromethane (40 mL) followed by triglyme (1.25 g, 7.06 mmol) and finally Hhfa (1.47 g, 7.06 mmol) were added after 10 min and the mixture was refluxed under stirring for 1 h. The excess of LiOH was filtered off. The obtained product did not crystallize and is liquid in nature. NMR analysis reports: δ_H (500 MHz, $CDCl_3$, 27 °C) 5.92 (s, 1H, CH_{HFA}), 3.734 (s, 4H, CH_2), 3.66 (m, 4H, CH_2), 3.54 (m, 4H, CH_2), 3.32 (s, 6H, CH_3) ppm; δ_C (125 MHz, $CDCl_3$, 27 °C) 176.55 (q, CO_{HFA}, ^2J(C,F)=32.6 Hz), 117.98 (q, $CF_{3\ HFA}$, ^1J(C,F)=287.8 Hz), 87.53 (CH_2), 71.05 (CH_2), 69.85 (CH_2), 69.56 (CH_2), 58.78 (CH_3) ppm. Elemental analysis for **3** ($LiC_{13}H_{19}F_6O_6$): Calc: C, 39.80; H, 4.88. Found: C, 39.61; H, 4.99.

Synthesis of Li(hfa)•tetraglyme (4). The Li(OH)•H_2O (0.385 g, 9.18 mmol) 30% excess was first suspended in dichloromethane (40 mL) followed by tetraglyme (1.57 g, 7.06 mmol) and finally Hhfa (1.47 g, 7.06 mmol) were added after 10 min and the mixture was refluxed under stirring for 1 h. The excess of LiOH was filtered off. The product obtained doesn't crystallize and is liquid in nature. NMR: δ_H (500 MHz, $CDCl_3$, 27 °C) 5.91 (s, 1H, CH_{HFA}), 3.68 (m, 8H, CH_2), 3.64 (m, 4H, CH_2), 3.54 (m, 4H, CH_2), 3.33 (s, 6H, CH_3) ppm; δ_C (125 MHz, $CDCl_3$, 27 °C) 176.52 (q, CO_{HFA}, ^2J(C,F)=32.9 Hz), 117,98 (q, $CF_{3\ HFA}$, ^1J(C,F)=287.4 Hz), 87.45(CH_2), 71.18 (CH_2), 69.85 (CH_2), 69.83(CH_2), 69.80 (CH_2), 58.80 (CH_3) ppm. Elemental analysis for **4** ($LiC_{15}H_{23}F_6O_7$): Calc: C, 45.93; H, 5.31. Found: C, 45.72; H, 5.14

X-ray crystallography experimental details. The molecular and crystal structure of the two complexes [Li_{12}(hfa)]$_{12}$•monoglyme•4H_2O] (**1**) and [Li_2(hfa)$_2$•diglyme•H_2O] (**2**), was investigated by means of single crystal X-ray diffraction at 100 K. Measurements for **1** were carried out with a Bruker APEX-II CCD diffractometer, while for **2** an Oxford Diffraction Excalibur diffractometer was used. In the two measurements the Cu-Kα radiation (λ = 1.54184 Å) was used. Data collections were performed with the program CrysAlis CCD[1] for **2** and with the Bruker APEX2 program for **1**.[2] Data reductions were carried out with the program CrysAlisPRO[3] for **2** and Bruker SAINT[4] for **1**. Finally, absorption corrections were performed with the program ABSPACK in CrysAlis RED for **2** and SADABS for **1**.[5] Structures were solved by using the SIR-2004 package[6] and subsequently refined on the F^2 values by the full-matrix least-squares program SHELXL-2013.[7]

Geometrical calculations were performed by PARST97,[8] and molecular plots were produced by the program Mercury (v3.7).[9]

In Table S1 crystal data and refinement parameters of the investigated structures are reported. The fluorine atoms bound to the carbon atom C(4) of the hfa anion, in **2**, as well as all the fluorine atoms bound to C(9) in **1** are disordered. Such a disorder was modelled, in the two crystals, by introducing three positions for each fluorine atom (occupancy factors: 0.34, 0.33, 0.33 in **1** and 0.45, 0.30, 0.25 in **2**). For the non-hydrogen atoms anisotropic thermal parameters were used. In all the two structures, the hydrogen atoms of the water molecules were found in the Fourier difference map and their positions were freely refined, while their thermal parameters were refined accordingly to the bound atoms.

Table S1. Crystallographic data and refinement parameters for $[Li_{12}(hfa)_{12}\bullet monoglyme\bullet 4H_2O]_n$ **(1)** and $[Li_2(hfa)_2\cdot(diglyme)\cdot H_2O]$ (**2**).

	$[Li_{12}(hfa)_{12}\bullet monoglyme\bullet 4H_2O]_n$ (**1**)	$[Li_2(hfa)_2\cdot(diglyme)\cdot H_2O]$ (**2**)
Empirical formula	$C_{64}H_{30}O_{30}F_{72}Li_{12}$	$C_{16}H_{18}O_8F_{12}Li_2$
Formula weight	2730.16	580.18
Temperature (K)	100	100
Wavelength (Å)	1.54184	1.54184
Crystal system, space group	Monoclinic, $P2_1/n$	Triclinic, P-1
Unit cell dimensions (Å, °)	a =17.930(1) b = 9.2458(5); β = 103.158(3) c = 30.375(2)	a = 9.427(1); α = 112.482(9) b = 11.433(1); β = 95.14(1) c = 12.245(1); γ = 92.239(9)
Volume ($Å^3$)	4903.3(5)	1210.6(2)
Z, D_c (mg/cm^3)	2, 1.849	2, 1.592
μ (mm^{-1})	2.073	1.631
F(000)	2676	584
Crystal size (mm)	0.25x0.20x0.18	0.35x0.30x0.28
θ range (°)	2.63 to 60.23	3.93 to 74.18
Reflections collected / unique	50824 / 7307	11683 / 4594
Data / parameters	7307 / 820	4594 / 359
Goodness-of-fit on F^2	1.040	1.085
Final R indices [I>2σ(I)]	R1 = 0.0605, wR2 = 0.1418	R1 = 0.0972, wR2 = 0.2580
R indices (all data)	R1 = 0.0722, wR2 = 0.1561	R1 = 0.1448, wR2 = 0.3398

Table S2. Selected bond distances (Å) and angles (°) for **1**.

Bond distances		Bond angles			
Li(1)-O(1W)	1.991(8)	O(1W)-Li(1)-O(1)	102.0(3)	O(6)-Li(4)-O(8)	86.4(3)
Li(1)-O(1)	2.012(7)	O(1W)-Li(1)-O(2)	102.8(3)	O(6)-Li(4)-O(9)	122(3)
Li(1)-O(2)	2.003(6)	O(1W)-Li(1)-O(3)	97.8(3)	O(6)-Li(4)-O(11)	112.0(3)
Li(1)-O(3)	2.015(6)	O(1W)-Li(1)-O(4)	111.5(3)	O(8)-Li(4)-O(9)	123.6(3)
Li(1)-O(4)	2.012(7)	O(1)-Li(1)-O(2)	88.9(3)	O(8)-Li(4)-O(11)	130.4(3)
Li(2)-O(2)	1.938(7)	O(1)-Li(1)-O(3)	85.6(3)	O(9)-Li(4)-O(11)	86.1(3)
Li(2)-O(4)	1.958(6)	O(1)-Li(1)-O(4)	146.4(4)		
Li(2)-O(5)	1.952(7)	O(2)-Li(1)-O(3)	159.3(4)	O(9)-Li(5)-O(10)	88.3(2)
Li(2)-O(7)	1.946(7)	O(2)- Li(1)-O(4)	84.2(3)	O(9)-Li(5)-O(11)	83.3(2)
Li(3)-O(5)	2.003(7)	O(3)-Li(1)-O(4)	89.6(3)	O(9)-Li(5)-O(12)	145.4(3)
Li(3)-O(2W)	2.010(8)			O(9)-Li(5)-O(1G)	108.0(3)
Li(3)-O(6)	2.011(7)	O(2)-Li(2)-O(4)	87.4(3)	O(10)-Li(5)-O(11)	154.8(3)
Li(3)-O(7)	2.006(7)	O(2)-Li(2)-O(5)	122.6(4)	O(10)-Li(5)-O(12)	84.4(2)
Li(3)-O(7)	2.007(7)	O(2)-Li(2)-O(7)	117.5(3)	O(10)-Li(5)-O(1G)	98.2(3)
Li(4)-O(6)	1.994(6)	O(4)-Li(2)-O(5)	122.2(3)	O(11)-Li(5)-O(12)	89.1(3)
Li(4)-O(8)	1.960(6)	O(4)-Li(2)-O(7)	122.7(3)	O(11)- Li(5)-O(1G)	107.0(3)
Li(4)-O(9)	1.974(6)	O(5)-Li(2)-O(7)	88.3(3)	O(12)-Li(5)-O(1G)	106.6(3)
Li(4)-O(11)	1.978(6)				
Li(5)-O(1G)	2.025(7)	O(2W)-Li(3)-O(5)	107.5(4)	$O(1)^{i}$-Li(6)-$O(3)^{i}$	84.9(3)
Li(5)-O(9)	2.039(6)	O(2W)-Li(3)-O(6)	99.2(3)	$O(1)^{i}$-Li(6)-O(10)	129.5(3)
Li(5)-O(10)	2.031(6)	O(2W)-Li(3)-O(7)	99.8(4)	$O(1)^{i}$-Li(6)-O(12)	124.0(3)
Li(5)-O(11)	2.022(6)	O(2W)-Li(3)-O(8)	103.9(3)	$O(3)^{i}$-Li(6)-O(10)	97.2(3)
Li(5)-O(12)	2.011(6)	O(5)-Li(3)-O(6)	90.3(3)	$O(3)^{i}$-Li(6)-O(12)	136.3(4)
Li(6)-$O(1)^{i}$	1.934(6)	O(5)-Li(3)-O(7)	85.2(3)	O(10)-Li(6)-O(12)	88.1(3)
Li(6)-$O(3)^{i}$	1.979(7)	O(5)-Li(3)-O(8)	148.6(4)		
Li(6)-O(10)	1.954(7)	O(6)-Li(3)-O(7)	161.0(4)		
Li(6)-O(12)	1.953(6)	O(6)- Li(3)-O(8)	84.7(3)		
		O(7)-Li(3)-O(8)	89.6(3)		

^{i} = x-0.5; -y+1.5; z-0.5

Table S3. Selected bond distances (Å) and angles (°) for **2**.

Bond distances		Bond angles	
Li(1)-O(1W)	1.96(1)	O(1W)- Li(1)- O(3)	110.5(5)
Li(1)-O(1)	2.03(1)	O(1W)- Li(1) O(1)	101.7(4)
Li(1)-O(2)	2.089(8)	O(1W) -Li(1)- O(4)	101.5(4)
Li(1)-O(3)	2.018(9)	O(1W)- Li(1)- O2	98.5(4)
Li(1)-O(4)	2.073(9)	O(1) -Li(1)- O(4)	91.8(4)
		O(1) -Li(1)- O(2)	86.2(4)
		O(3) -Li(1) -O(2)	85.0(3)
		O(3) -Li(1)- O(4)	86.1(3)
		O(3)- Li(1)- O(1)	147.5(5)
		O(4) -Li(1)- O(2)	159.9(5)
Li(2)-O(2)	1.983(9)	O(2)- Li(2)- O(5)	97.0(5)
Li(2)-O(3)	1.976(9)	O(2)- Li(2)- O(6)	117.9(5)
Li(2)-O(5)	2.09(1)	O(2)- Li(2)- O(7)	108.3(5)
Li(2)-O(6)	2.051(9)	O(3)- Li(2)- O(2)	89.0(3) .
Li(2)-O(7)	2.03 (1)	O(3)- Li(2) O(5)	92.7(4)
		O(3)- Li(2)- O(6)	152.4(5)
		O(3)- Li(2) -O(7)	98.6(5)
		O(6)- Li(2)- O(5)	78.6(4)
		O(7)- Li(2)- O(5)	152.3(5)
		O(7)-Li(2)- O(6)	79.7(3)
Intermolecular Interactions			
X-H···Y	X···Y (Å)	H···Y (Å)	X-H···Y (°)
O(1w)-H(1wa)···O(1)[1]	2.824(6)	1.99(7)	166(6)
O(1w)-H(1wa)···O(4)[1]	2.841(5)	2.14(5)	140(5)

[1]= -x,-y+2,-z+2

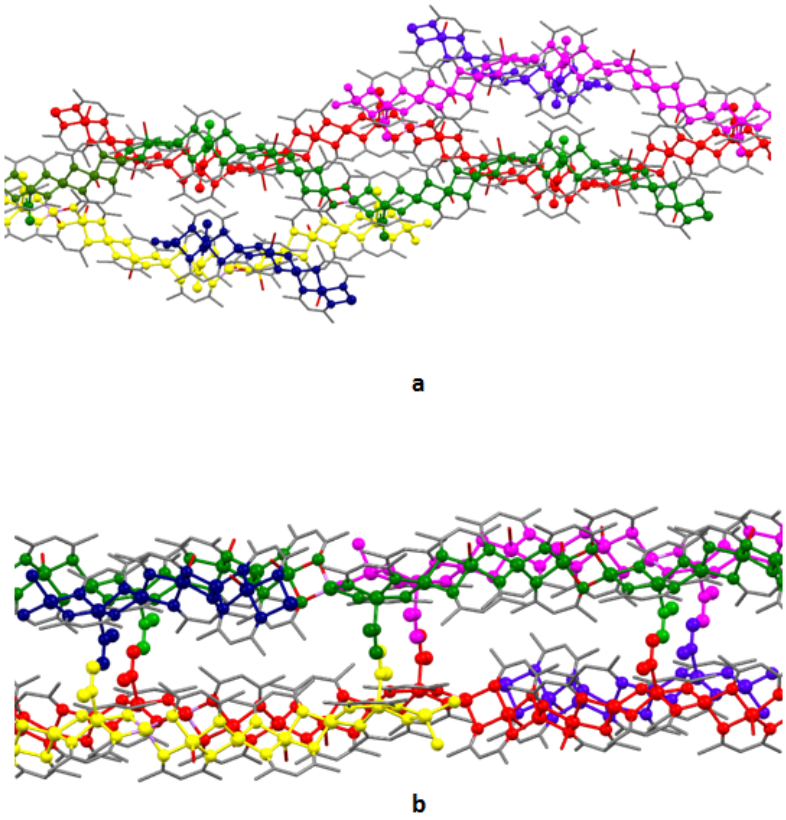

Fig. S1. Ball and stick view of the $[Li_{12}(hfa)_{12}$•monoglyme•$4H_2O]_n$ polymeric chains. a) View along the 'a' axis direction (different colors have been used to highlight the wave-like motif described by the Li-O_{hfa} moieties). b) View highlighting the Li-monoglyme-Li bonds which assembles the Li-O_{hfa} polymeric chains.

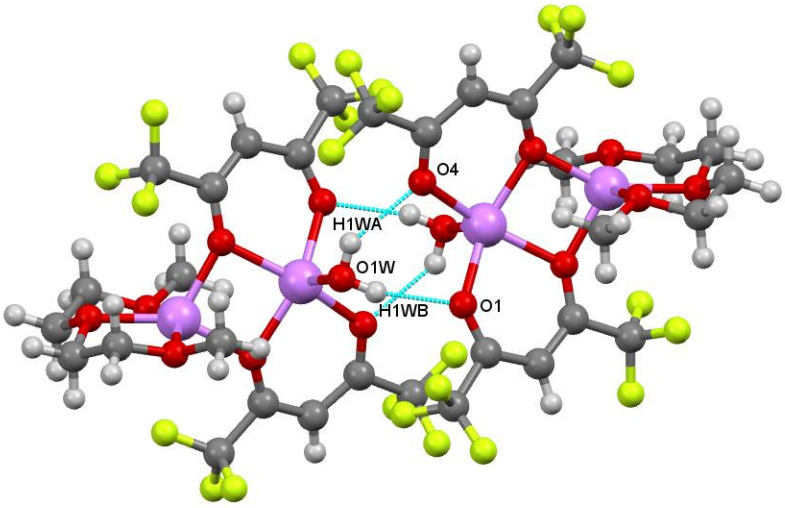

Fig. S2. Ball and stick view of the $[Li_2(hfa)_2$•diglyme•$H_2O]$ dimer.

The FT-IR transmittance spectra of the complexes **2**, **3** and **4** (Fig. S3) show the presence of band around 3500 cm^{-1}, due to OH stretching, thus confirming the coordination of water molecules to the the complexes. The peaks around 1657 and 1530 cm^{-1} (**1, 2, 3 and 4**) are associated with the C=O stretching and with C=C stretching vibrations, and are typical of the β-diketonate framework.[7-10] Peaks observed in the 1000-1300 cm^{-1} range are characteristic of the polyether C-O bending and/or stretching overlapped with the C-F stretching features. In addition, the glyme modes appear around 1004, 953, and 842 cm^{-1} (**1, 2, 3 and 4**). In the spectral range of 2800-3000 cm^{-1}, it is possible to find the C-H glyme stretching modes overlapped with nujol features. The nujol shows also peaks at 1461 and 1377 cm^{-1}.

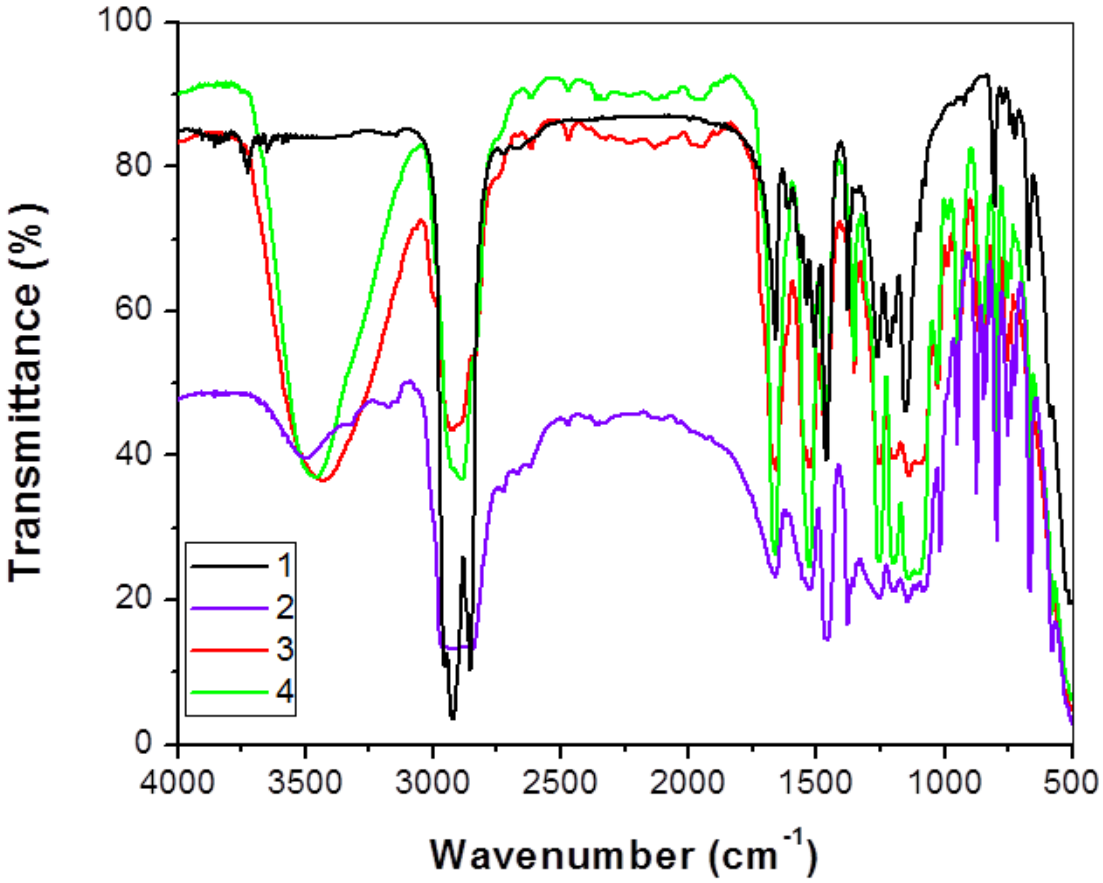

Fig. S3. FT-IR spectra of adducts **1, 2, 3** and **4**

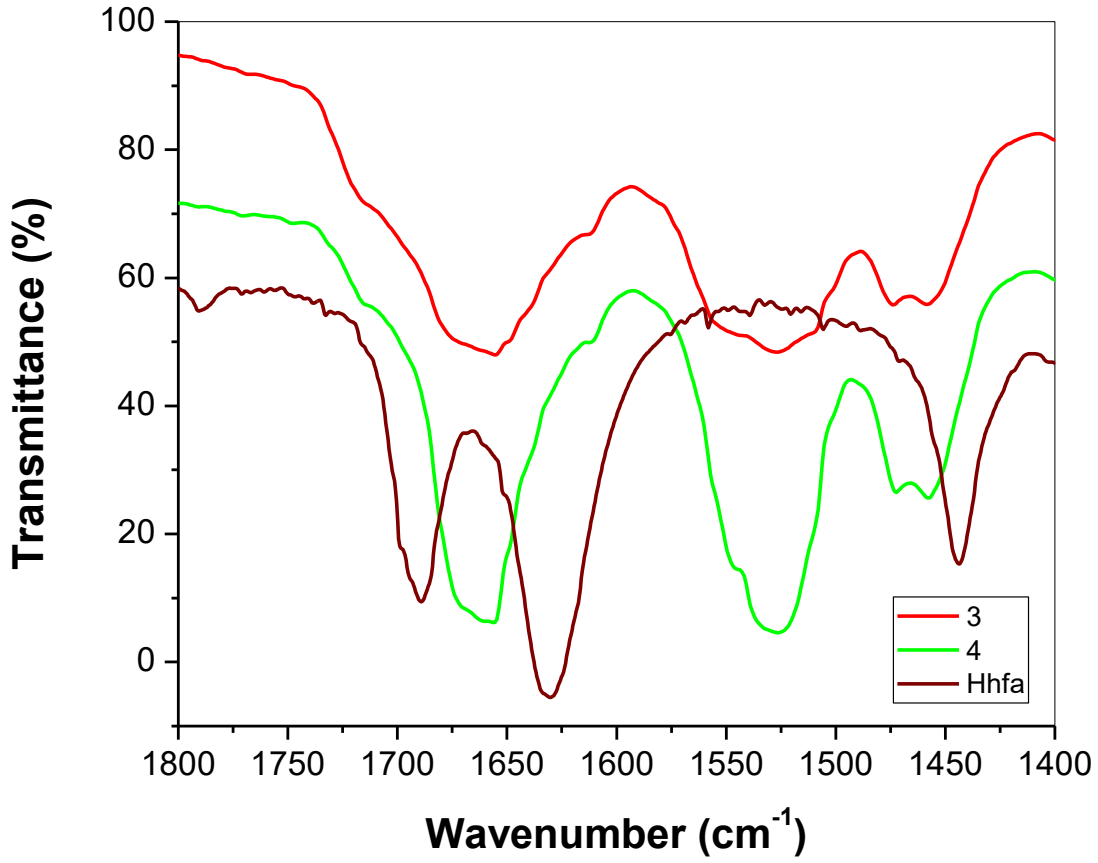

Fig. S4. FT-IR spectra of **3** and **4** vs. the free Hhfa ligand in the carbonyl range.

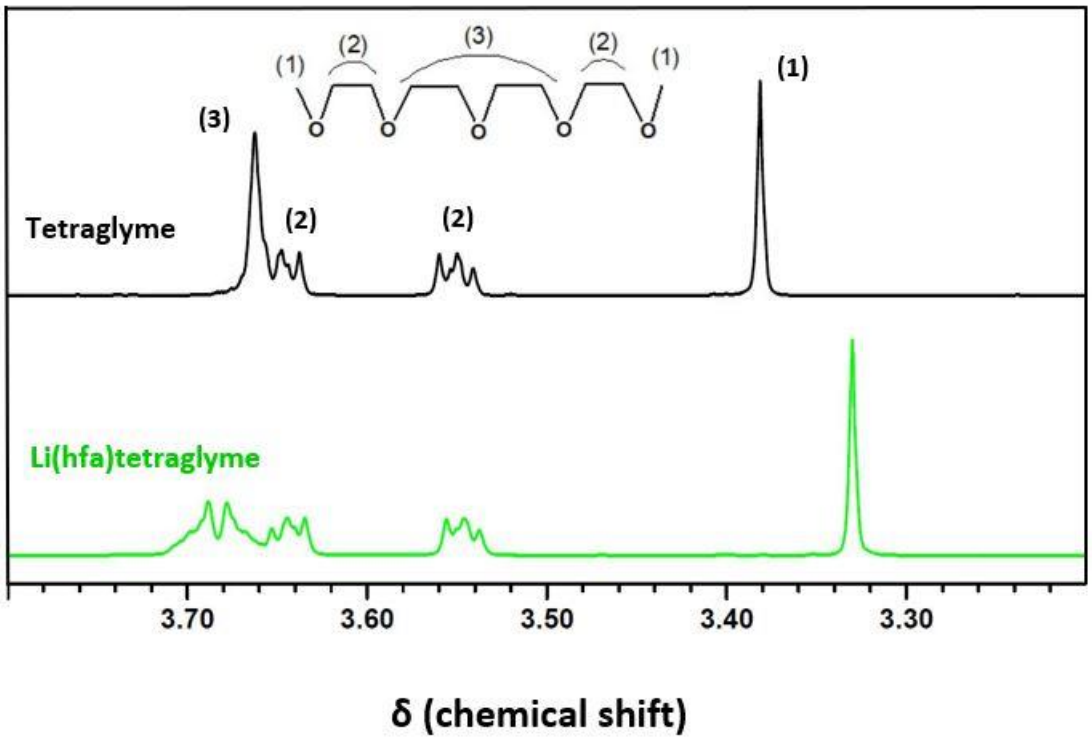

Fig. S5. Comparison of ^{1}H-NMR spectra (polyether region) of tetraglyme (——) and Li(hfa)tetraglyme (——).

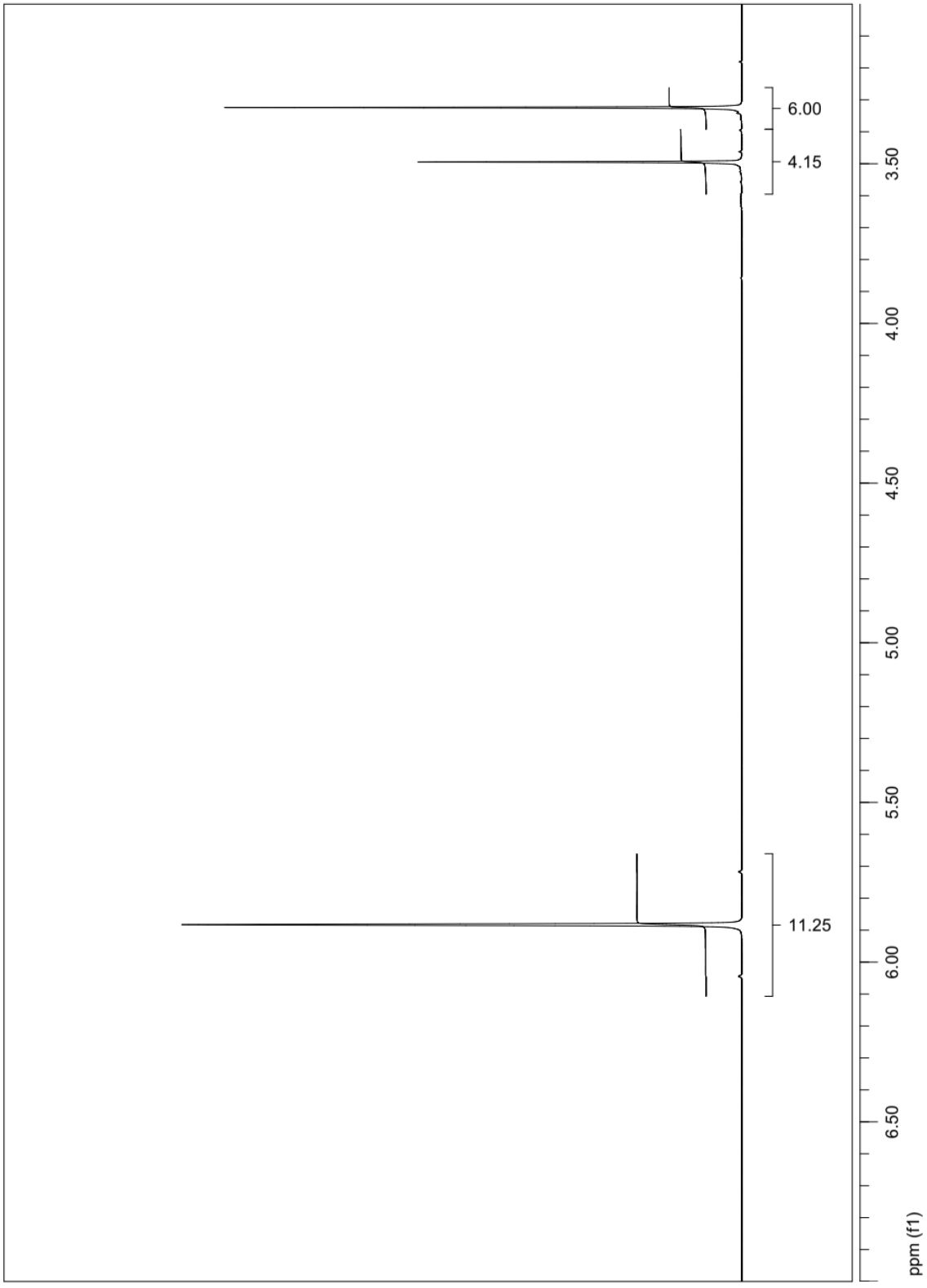

Fig. S6. ^{1}H-NMR spectrum of **1** (CD_3CN, 500 MHz, 27 °C).

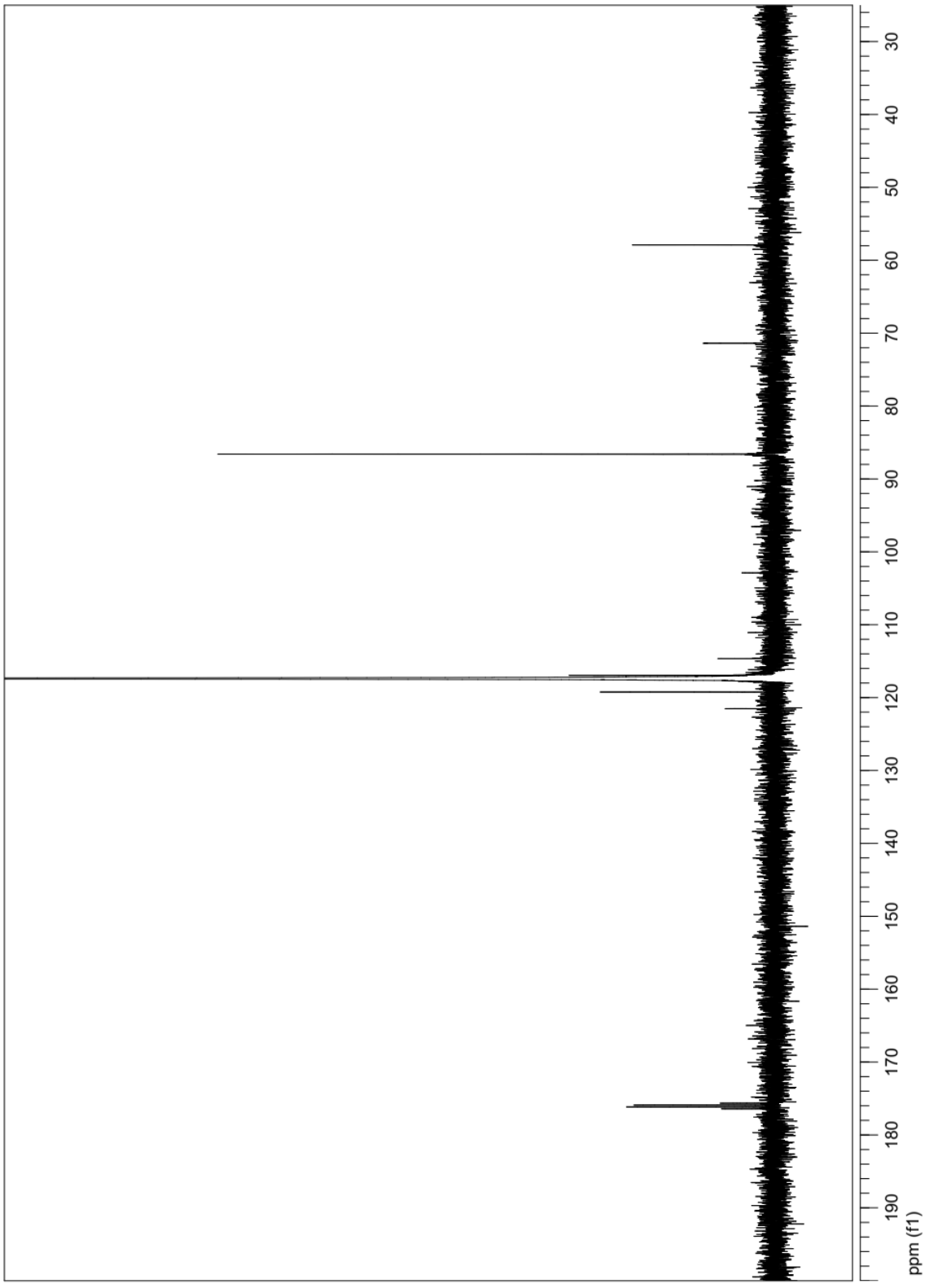

Fig. S7. ^{13}C-NMR spectrum of **1** (CD_3CN, 125 MHz, 27 °C)

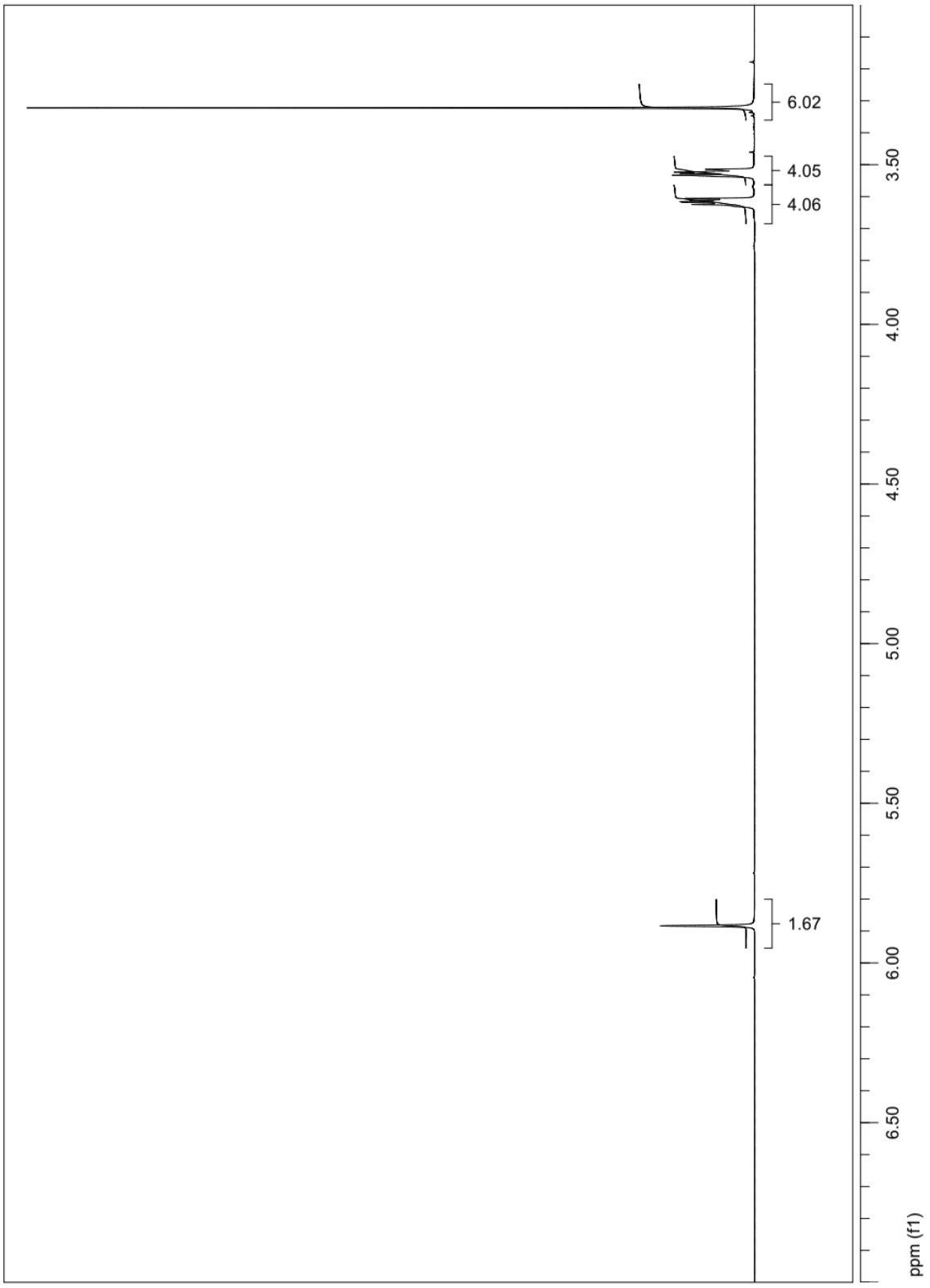

Fig. S8. ^{1}H-NMR spectrum of **2** (CD_3CN, 500 MHz, 27 °C).

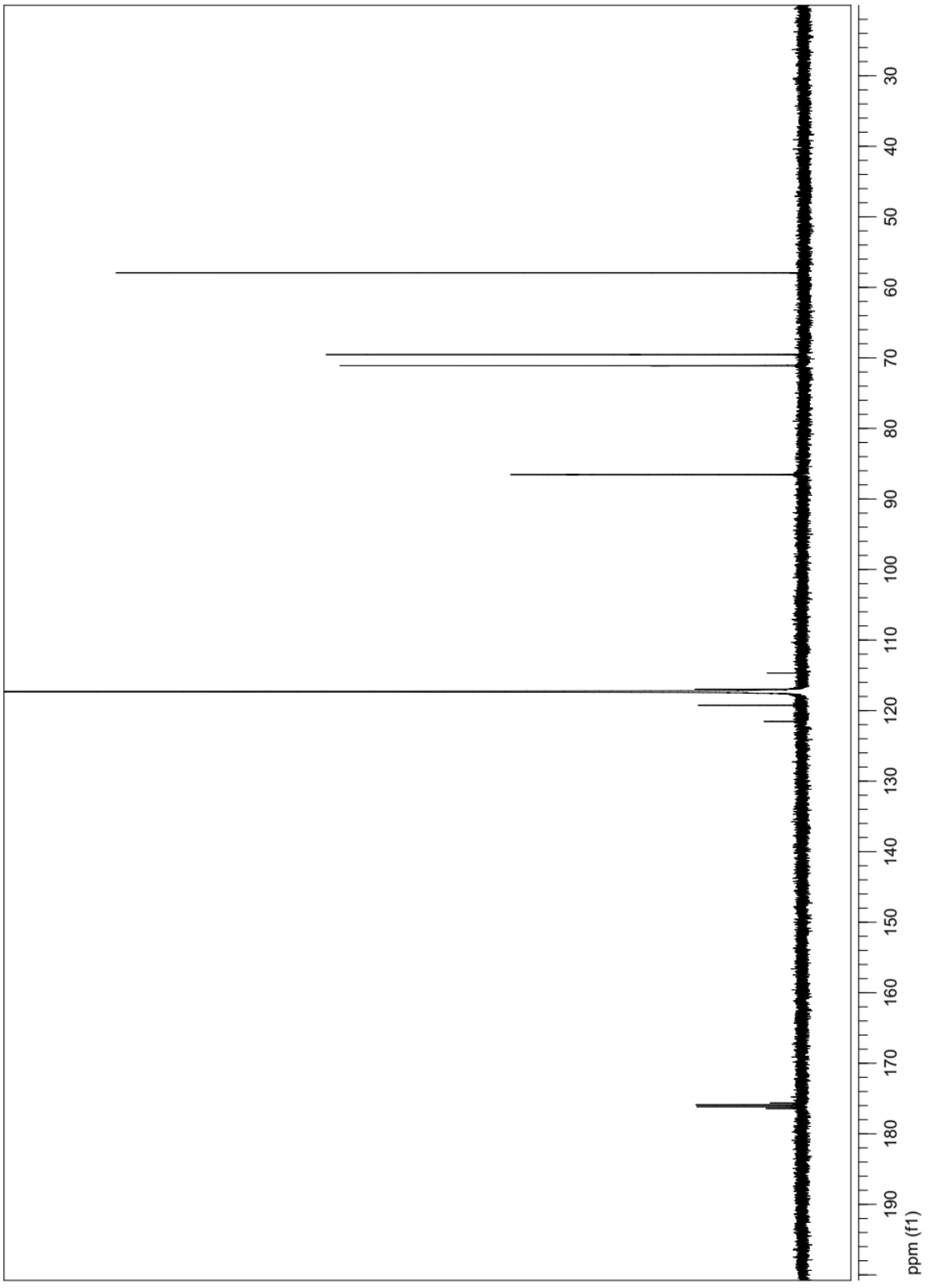

Fig. S9. ^{13}C-NMR spectrum of **2** (CD_3CN, 125 MHz, 27 °C).

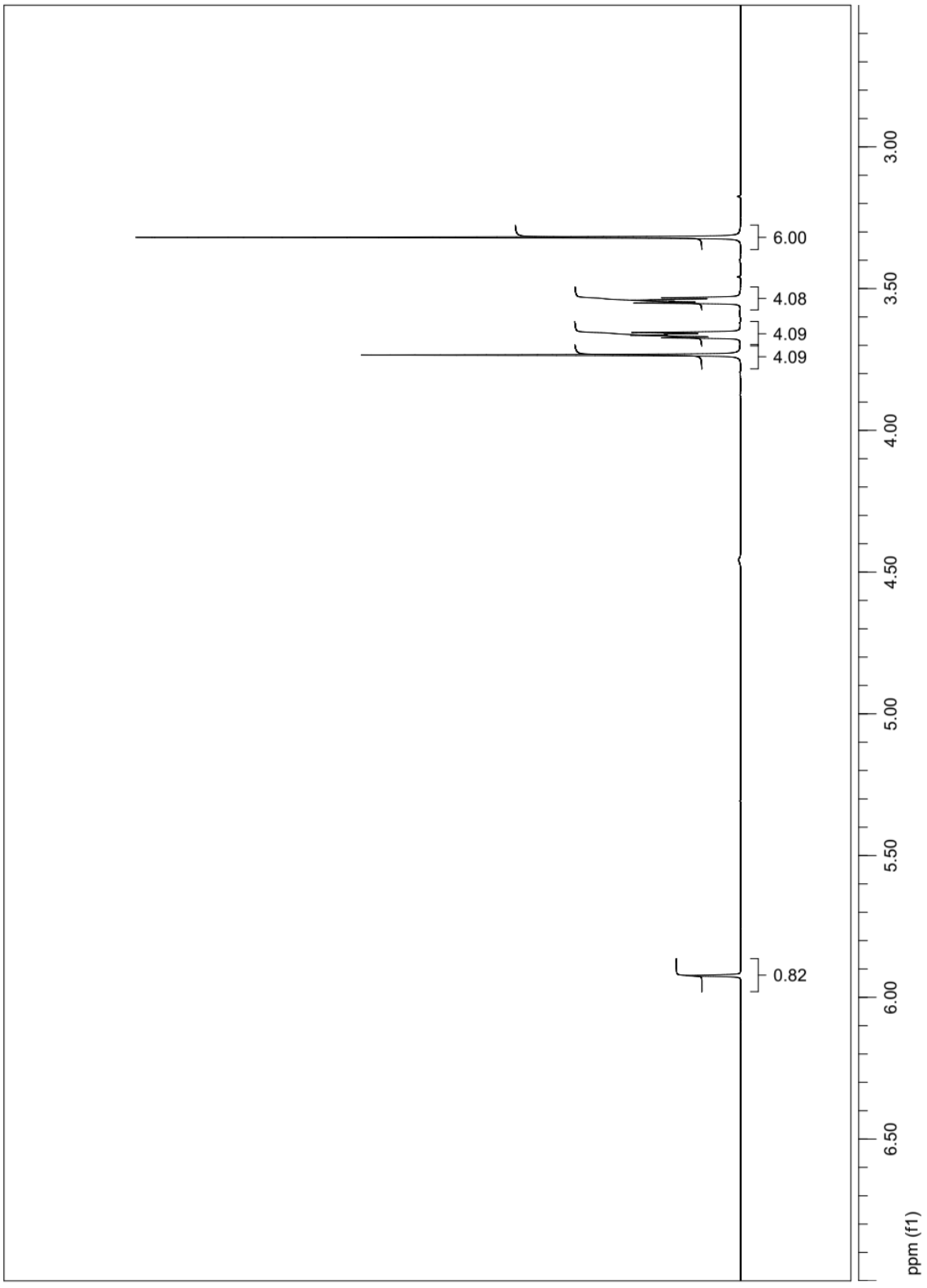

Fig. S10. ^{1}H-NMR spectrum of **3** ($CDCl_3$, 500 MHz, 27 °C).

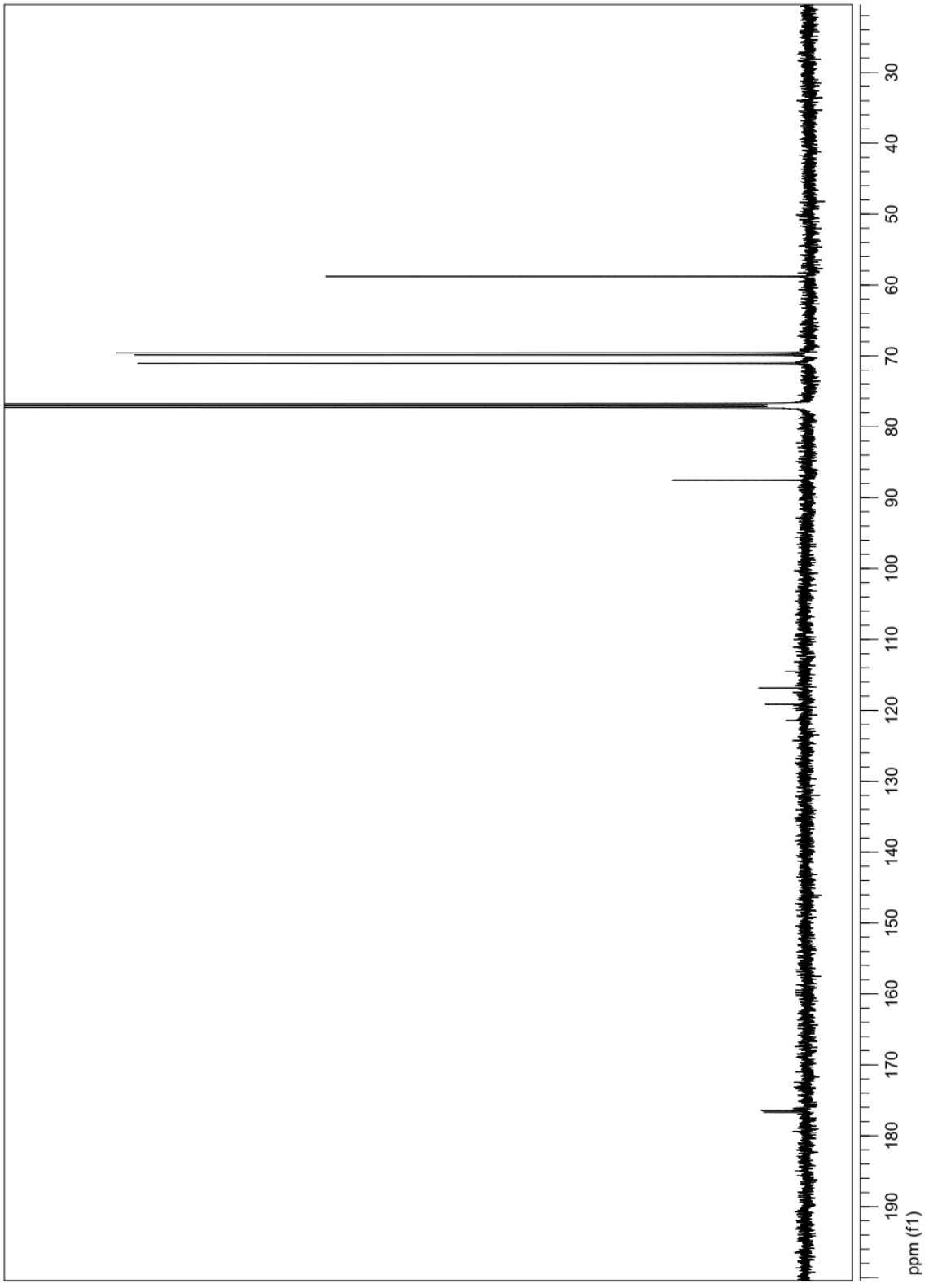

Fig. S11. ^{13}C-NMR spectrum of **3** ($CDCl_3$, 125 MHz, 27 °C).

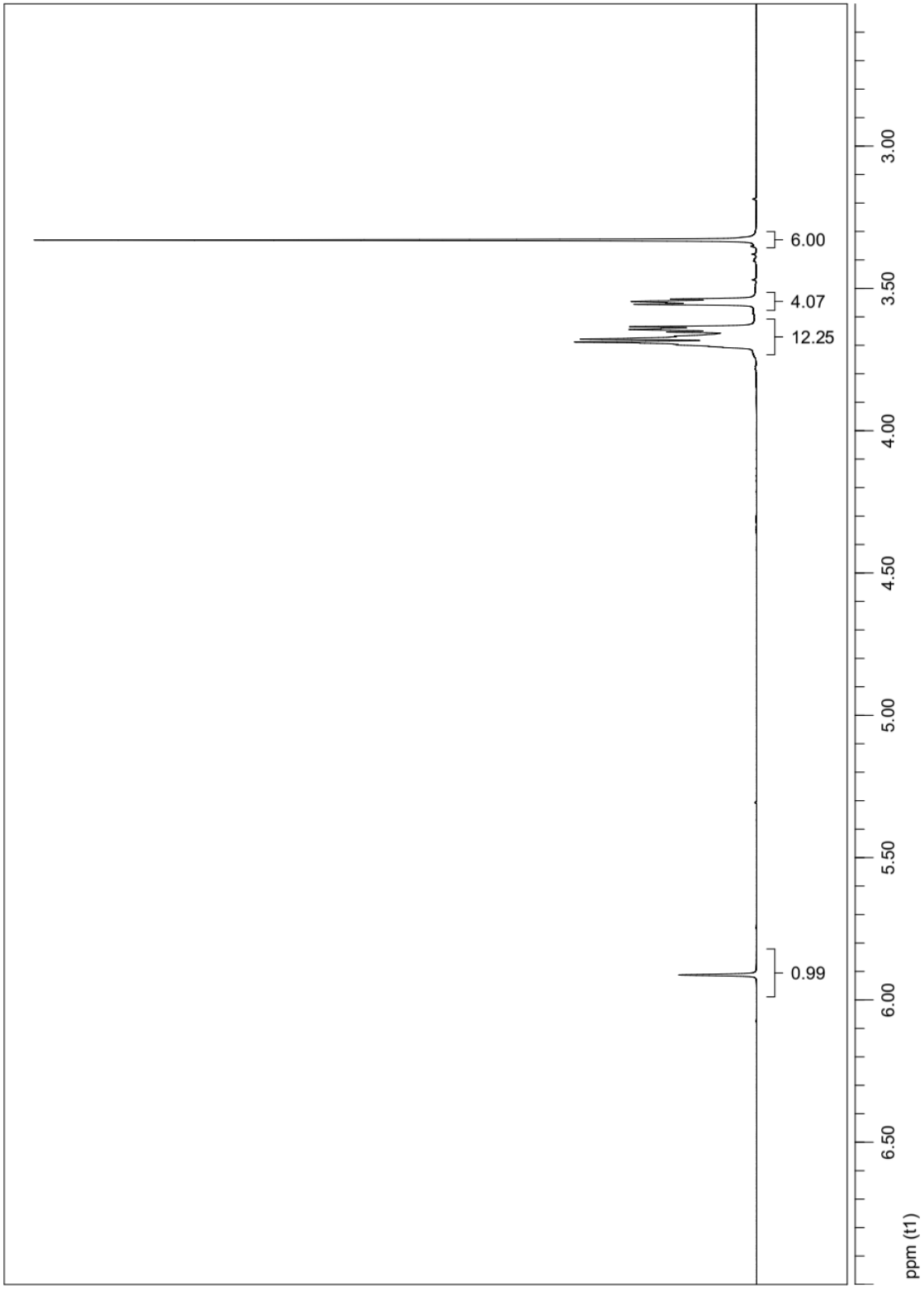

Fig. S12. ^{1}H-NMR spectrum of **4** ($CDCl_3$, 500 MHz, 27 °C).

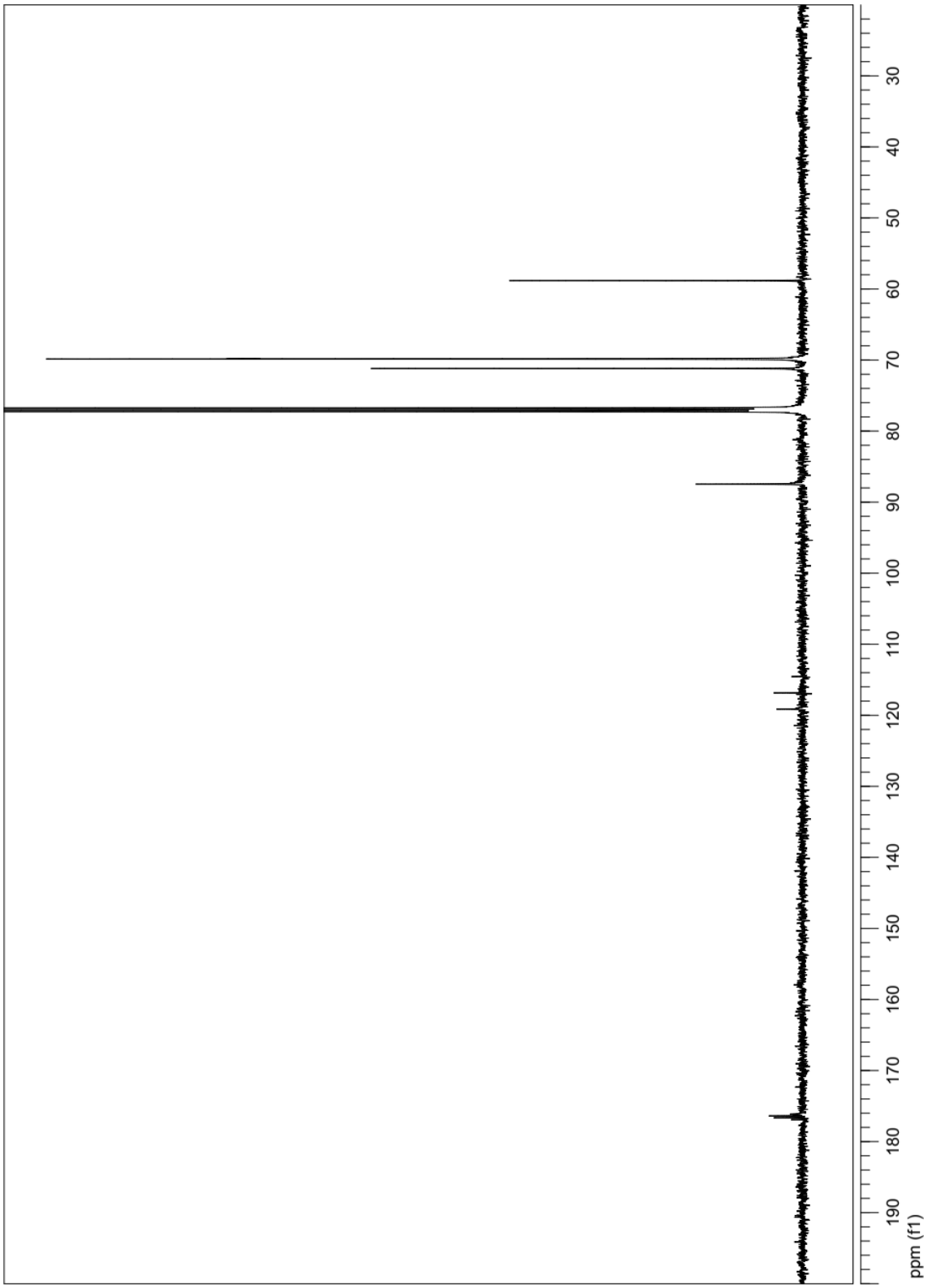

Fig. S13. ^{13}C-NMR spectrum of **4** ($CDCl_3$, 125 MHz, 27 °C).

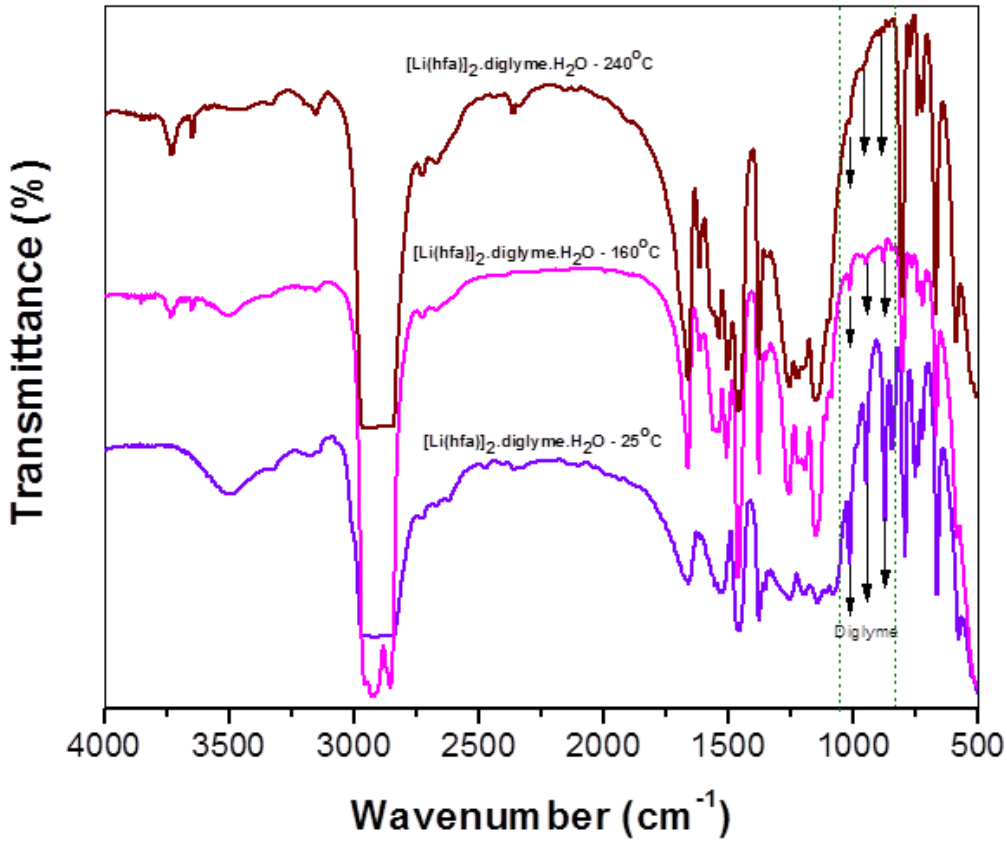

Fig. S14. FT-IR spectra of **2** recorded at 25 ºC, 160 ºC and 240 ºC.

Film deposition. Pulsed injection MOCVD (PI-MOCVD) depositions were carried out in a customized vertical reactor under 7 torr pressure. The films were deposited on C-Al_2O_3 at 775 °C. The multisource precursor mixture was prepared dissolving the $[Li_{12}(hfa)_{12}$•monoglyme•$4H_2O]_n$ and the $Nb(tmhd)_4$ precursors in a 2:1 ratio in monoglyme. The evaporation temperature was fixed at 220 °C. Argon was used as carrier gas and oxygen was used as the reactant gas, which was introduced in the main flow in proximity to the reaction zone.

References

[1] CrysAlisPro, Agilent Technologies, 2011

[2] BRUKER APEX2, Bruker AXS Inc., Madison, Wisconsin, USA, 2012

[3] CrysAlisPro 1.171.39.46, Rigaku OD, 2018

[4] BRUKER SAINT, Bruker AXS Inc., Madison, Wisconsin, USA, 2012

[5] L. Krause, R. Herbst-Irmer, G. M. Sheldrick and D. Stalke, *J. Appl. Cryst.*, 2015, **48**, 3-10.

[6] M. C. Burla, R. Caliandro, M. Camalli, B. Carrozzini, G. L. Cascarano, L. Da Caro, C. Giacovazzo and G. Polidori, R. Spagna, *J. Appl. Cryst.*, 2005, **38**, 381-388.

[7] T. Gruene, H. W. M. Hahn, A. V. Luebben, F. Meilleur and G. M. Sheldrick, *J. Appl. Cryst.*, 2014, **47**, 462-466.

[8] M. Nardelli, *J. Appl. Cryst.*, 1995, **28**, 659.

[9] C. F. Macrae, I. J. Bruno, J. A. Chisholm, P. R. Edgington, P. McCabe, E. Pidcock, E. Rodriguez-Monge, R. Taylor, V. De Streek, P. A. J. Wood, *J. Appl. Cryst*., 2008, **41**, 466-470.